Structure
Article

The C-Terminal BAG Domain of BAG5 Induces Conformational Changes of the Hsp70 Nucleotide-Binding Domain for ADP-ATP Exchange

Akihiko Arakawa,[1,2] Noriko Handa,[2] Noboru Ohsawa,[2] Meiri Shida,[1,2,4] Takanori Kigawa,[2,3] Fumiaki Hayashi,[2] Mikako Shirouzu,[2] and Shigeyuki Yokoyama[1,2,*]
[1]Department of Biophysics and Biochemistry, Graduate School of Science, The University of Tokyo, 7-3-1 Hongo, Bunkyo-ku, Tokyo 113-0033, Japan
[2]RIKEN Systems and Structural Biology Center, 1-7-22 Suehiro-cho, Tsurumi, Yokohama 230-0045, Japan
[3]Tokyo Institute of Technology, 4259 Nagatsuta-cho, Midori-ku, Yokohama 226-8502, Japan
[4]Present address: Chugai Pharmaceutical Co., Ltd., 1-135 Komakado, Gotemba, Shizuoka 412-8513, Japan
*Correspondence: yokoyama@biochem.s.u-tokyo.ac.jp
DOI 10.1016/j.str.2010.01.004

SUMMARY

ADP-ATP exchange by the molecular chaperone Hsp70 is enhanced by several cochaperones. BAG5 consists of five BAG domains and associates with the nucleotide-binding domain (NBD) of Hsp70. The overexpression of BAG5 in the cytosol reportedly disturbs Hsp70-mediated protein refolding and induces Parkinson's disease. In the present study, we found that the fifth BAG domain (BD5) of BAG5 is responsible for the interaction between Hsp70 and BAG5. We also determined the crystal structures of the BD5•NBD complex. BD5 binding caused two different types of NBD conformational changes, which both disrupted the nucleotide-binding groove. In fact, BD5 reduced the affinity of the NBD for ADP. Moreover, BD5, as well as the full-length BAG5, accelerated Hsp70-mediated refolding in an in vitro assay. Therefore, BAG5 can function as the nucleotide exchange factor of Hsp70 for the enhancement of protein refolding.

INTRODUCTION

The 70 kDa heat shock proteins (Hsp70s) are ubiquitous and abundant molecular chaperones for all organisms. They include the stress-induced Hsp70 and the housekeeping Hsc70, which assist in the correct folding of denatured and/or nascent proteins, to prevent protein aggregation (Bukau et al., 2006; Hartl and Hayer-Hartl, 2002; Mayer and Bukau, 2005). Hsp70s are composed of the N-terminal nucleotide-binding domain (NBD) and the C-terminal substrate-binding domain (SBD) (Figure 1A). Hsp70s in the ATP-bound state catch and release their substrates rapidly, while Hsp70s in the ADP-bound state seize them firmly. By cycling between the ATP- and ADP-bound states, Hsp70s exert their chaperone activity (Bukau and Horwich, 1998). The ATP hydrolysis activity of Hsp70s converts the ATP-bound state to the ADP-bound state. The J cochaperones recruit the substrate to the ATP-bound Hsp70s and enhance the ATP hydrolysis activity (Misselwitz et al., 1998; Walsh et al., 2004). After ATP hydrolysis, Hsp70s can release ADP by themselves, via the interaction between the NBD and SBD (Jiang et al., 2005), but the release rate is quite slow. Therefore, in this step, Hsp70s use nucleotide exchange factors (NEFs), such as GrpE (Liberek et al., 1991) in bacteria and the Hsp110s (Andreasson et al., 2008; Dragovic et al., 2006; Raviol et al., 2006; Shaner et al., 2006) and HspBP1/Fes1/Sls1 (Kabani et al., 2002) in eukaryotes. The interaction of the NEFs with the NBD facilitates the release of ADP, accelerates the ATP cycle, and activates the refolding activity of Hsp70 (Harrison et al., 1997; Polier et al., 2008; Schuermann et al., 2008; Shomura et al., 2005).

The Bcl-2-associated athanogene (BAG) family is one of the Hsp70 NEF families and is evolutionally conserved among eukaryotes (Kabbage and Dickman, 2008; Takayama and Reed, 2001). The human BAG family consists of six members, BAG1, BAG2, BAG3 (CAIR-1/Bis), BAG4 (SODD), BAG5, and BAG6 (Scythe/BAT3) (Takayama et al., 1995, 1999; Thress et al., 1998). The BAG domain (BD) of BAG1 is composed of 112 residues and forms three almost parallel α helices (Briknarová et al., 2001). In the early stage of research, the effect of BAG1 on the chaperon activity of Hsp70 was not clarified and reported to be either positive (Höhfeld and Jentsch, 1997; Gassler et al., 2001) or negative (Bimston et al., 1998; Nollen et al., 2001; Takayama et al., 1997). However, the crystal structure of a complex between the BAG1 BD and the Hsc70 NBD revealed that the BAG1 BD induces the conformational change of the NBD to the open state and facilitates ADP release (Sondermann et al., 2001). The BD is thereby responsible for the NEF activity of BAG1. In contrast, BAG2 lacks the BD, but contains the brand new BAG (BNB) domain, which is also composed of three non-parallel α helices (Xu et al., 2008). Binding of the BAG2 BNB domain to Hsc70 NBD causes a different type of conformational change in the NBD, which also facilitates ADP dissociation (Xu et al., 2008). In contrast, BAG3, BAG4, and BAG5 conserve the BD, which consists of three parallel α helices, but is about 25 residues shorter than the BAG1 BD (Figure 1B) (Briknarová et al., 2002; Brockmann et al., 2004). No NBD complex structure is currently available for these shorter BDs.

BAG5 is a unique BAG protein, because BAG5 contains five shorter BDs in tandem (Figure 1A) (Briknarová et al., 2002). BAG5-overexpression state reduces the cellular Hsp70-mediated refolding activity. In addition to the BAG5-induced inhibition of

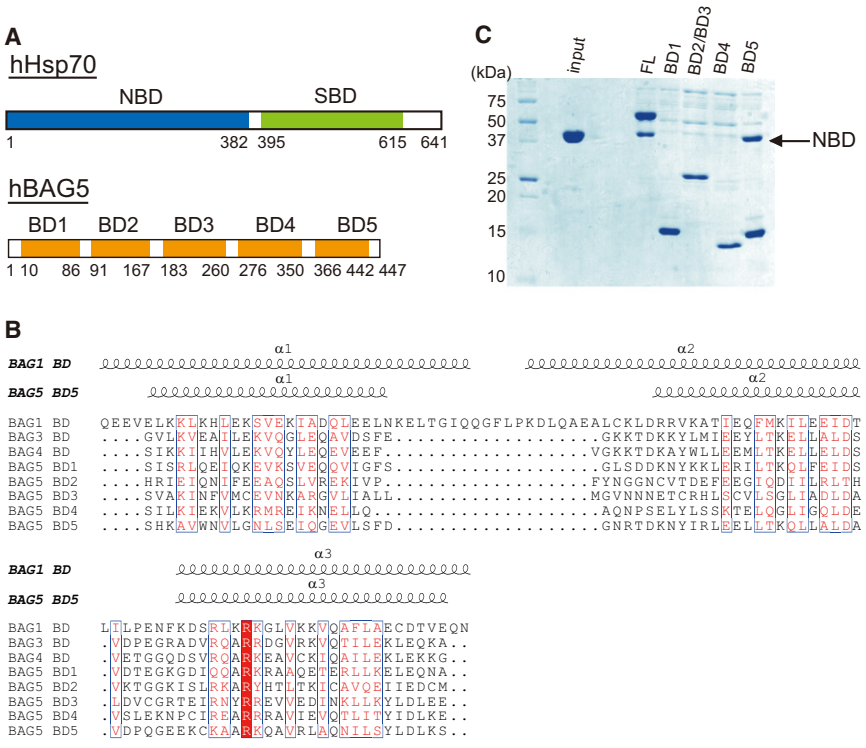

Figure 1. Crystal Structure of the BAG5 BD5 and Hsp70 NBD Complex

(A) Domain structures of human Hsp70 and BAG5. Hsp70 is composed of the NBD (cyan) and SBD (green), and BAG5 has five BDs (orange), designated as BD1, BD2, BD3, BD4, and BD5.

(B) In vitro pull-down assay, using the His-BAG5 full-length (FL), BD1 (residues 1–89), BD2–3 (residues 86–260), BD4 (residues 275–350), and BD5 (residues 341–447) and the purified Hsp70 NBD (residues 1–388). In the lane labeled "input," only purified Hsp70 NBD was loaded.

(C) Secondary structures of the BAG1 BD and BAG5 BD5, and sequence alignment of the BDs in human BAG1, BAG3, BAG4, and BAG5.

(D) Crystal structure of the BD5•NBD complex. The asymmetric unit contains two complexes, designed as complexes A and B. The green and cyan ribbon diagrams represent the Hsp70 NBD, and the magenta and orange ribbon diagrams represent the BAG5 BD5. Molecular graphics were generated and rendered using the program PyMOL (DeLano Scientific). As shown Figure S1, we detected no nucleotide in the BD5•NBD complex.

parkin E3 ligase, the overexpression of BAG5 promotes protein aggregation in dopaminergic neurons and causes the neurodegeneration associated with endoplasmic reticulum stress, which leads to Parkinson's disease (Chung and Dawson, 2004; Kalia et al., 2004). In contrast, BAG5 is expressed in multiple tissues in rat and human (Kalia et al., 2004) and its function in the normal state has not been elucidated.

In the present study, we found that the fifth BD (BD5) of BAG5 is responsible for the binding of BAG5 to the Hsp70 NBD. We determined the crystal structure of the BD5•NBD complex. There were two complexes in the asymmetric unit. In one BD5•NBD complex, the NBD structure is in the open state, which is similar to that in the BAG1 BD•NBD complex. In the other BD5•NBD complex, the NBD structure is distinct, and the pocket for ADP/ATP binding is distorted. Actually, it was demonstrated that the BD5 reduced the affinity of the NBD for ADP. Therefore, either or both of the structures may contribute to the rapid dissociation of ADP from the NBD. Moreover, we found that the full-length BAG5, as well as BD5, enhanced the refolding activity of Hsp70. Therefore, we concluded that BAG5 assists Hsp70-mediated refolding activity as the NEF, through the interaction between the BD5 and the NBD.

RESULTS AND DISCUSSION

The BAG5 BD5 Associates with the Hsp70 NBD Fragment

BAG5 reportedly interacts with the NBD, but not with the SBD, of Hsp70 in the cytosol (Kalia et al., 2004). However, it has remained elusive how many and which of the five BDs participate in binding to the NBD. Therefore, we prepared fragments of BD1 (residues 1–89), BD2–3 (residues 86–260), BD4 (residues 275–350), and BD5 (residues 341–447), as well as the full-length protein (BAG5 FL; residues 1–447), and performed in vitro pull-down assays with the Hsp70 NBD (residues 1–388). First, we demonstrated that the purified BAG5 FL associated with the NBD fragment in vitro. Moreover, as shown in Figure 1C, the BAG5 BD5 as well as the BAG5 FL pulled down the NBD, whereas the other BDs did not. Therefore, the BD5 binds to the NBD most strongly among the BAG5 BDs.

Crystal Structure of the BD5•NBD Complex

Next, we mixed the recombinant fragments of the Hsp70 NBD and the BAG5 BD5, and purified the BD5•NBD complex. The

elution pattern of the BD5•NBD complex in the gel-filtration chromatography indicated that the complex contains one molecule of each protein. An HPLC analysis revealed that neither ATP nor ADP was detected with the BD5-bound NBD, whereas ADP was detected with the recombinant NBD fragment itself (see Figure S1 available online). Therefore, the purified complex was composed of the BD5 and the NBD in the nucleotide-free state. We crystallized this sample and collected a 2.3 Å native data set. The crystal structure was solved by the molecular replacement method, using the program MOLREP (CCP4, 1994). The NBD structure in the complex with the BAG1 BD (PDB ID: 1HX1) (Sondermann et al., 2001) and the BD5 structure created by SWISS-MODEL (http://swissmodel.expasy.org//SWISS-MODEL.html) were used as the search models. After remodeling the residues of the BD5•NBD complex, we refined it to an R/R_{free} of 21.8/28.1. In this crystal, the asymmetric unit contains two complexes, which are designated as complexes A and B (Figure 1D).

Comparisons of the BD Structures

As mentioned above, the BDs of BAG5 and BAG3 are shorter than the BAG1 BD, but are similar to the BAG4 BD (Figure 1B). First, the present structures of the BD5 complexed with the NBD were compared with the NMR solution structure of the BAG1 BD (PDB ID: 1I6Z) (Briknarová et al., 2001) and the crystal structure of the BAG1 BD complexed with the NBD. Actually, helices α1 and α2 in the BD5 are shorter by 12 and 11 residues, respectively, than those in the BAG1 BD, while helix α3 is only two residues shorter (Figure 2A). In contrast, the positions and directions of the three helices in the BD5 are the same as those in the BAG1 BD. In contrast, the present BD5 structures are very similar to the NMR solution structure of the BAG4 BD (PDB ID: 1M62) (Briknarová et al., 2002) (Figure 2B).

Next, we determined the NMR solution structures of the murine BAG5 BD1 (Figure 2C), human BAG5 BD4 (Figure 2D), and murine BAG3 BD (Figure 2E). All of these structures exhibited three short α helices, as in those of the BAG4 BD and the BAG5 BD5. In contrast, the BAG3 BD structure superimposed very well onto the BAG5 BD5 structure (Figure 2H) and the BAG5 BD1 and BD4 assumed almost the same overall structures as that of the BD5, although the binding of the BD1 or BD4 to the NBD was not detected. The root mean square deviations of the BAG5 BD1 and BD4 structures from the BD5 structure in complex A are no more than 1.1 Å (Figure 2F) and 1.5 Å (Figure 2G), respectively.

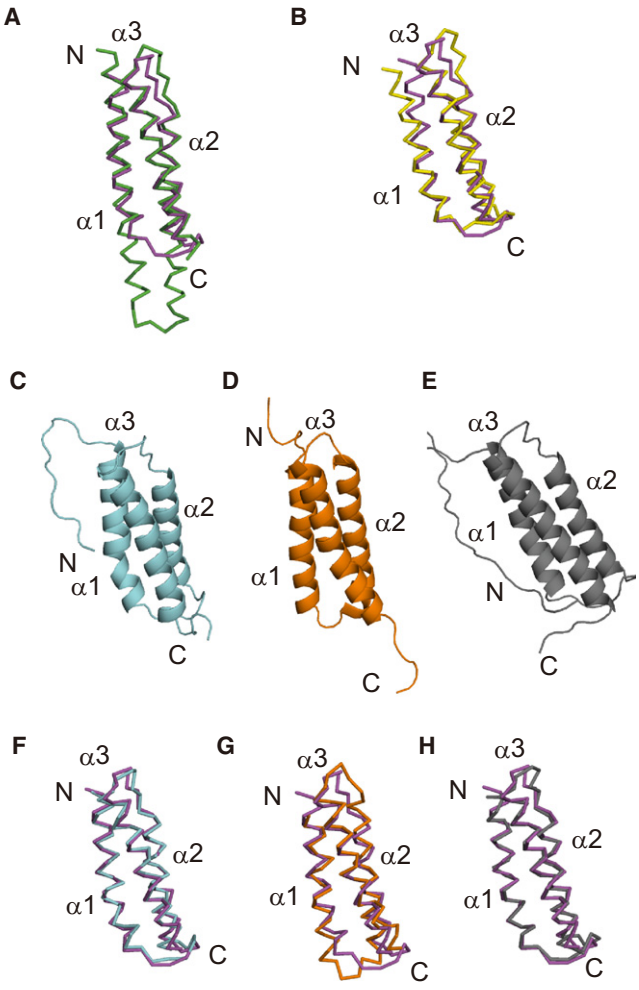

Figure 2. Structural Comparison of the BDs

(A) Comparison of the BAG1 BD (green) and the BAG5 BD5 (magenta).
(B) Comparison of the BAG4 BD (yellow) and the BAG5 BD5.
(C) Solution structure of the BAG5 BD1, represented by a cyan ribbon diagram.
(D) Solution structure of the BAG5 BD4, represented by an orange ribbon diagram.
(E) Solution structure of the BAG3 BD, represented by a gray ribbon diagram.
(F) Comparison of the BAG5 BD1 (cyan) and BD5.
(G) Comparison of the BAG5 BD4 (orange) and BD5.
(H) Comparison of the BAG3 BD (gray) and the BAG5 BD5.

Interaction between the BD5 and the NBD

The BAG5 BD5 as well as the BAG1 BD interacts with the NBD via helices α2 (residues 393–411) and α3 (residues 418–442) (Figures 3A–3D). In both complexes A and B, the negatively charged side chains of Glu399, Glu400, and Asp410 from helix α2 of the BD5 interact with the positively charged side chains of Lys257, Arg258, Arg261, Arg262, and Arg269 in the NBD (Figures 3A and 3C), while the side chains of Arg424, Lys425, and Gln432 from helix α3 of the BD5 interact with the negatively charged side chains of Asp285 and Asp292 and the hydroxyl groups of Ser286 and Tyr294 in the NBD (Figures 3B and 3D). Next, we mutated Glu399, Glu400, Asp410, Arg424, and Gln432 in the BD5 (residues 361–447) to alanine and performed in vitro pull-down assays. The D399A and D400A mutations reduced the NBD binding, and the D410A, R424A, and Q432A mutations abolished it (Figure 3F). Therefore, these residues of the BD5 are important for the interaction with the NBD. Furthermore, Glu399, Glu400, Asp410, Arg424, and Gln432 of the BD5 are conserved in the BAG3 and BAG4 BDs (Figure 3E), suggesting that their NBD binding modes are almost the same as that of the BAG5 BD5. In contrast, the other BAG5 BDs lack a few of the NBD-interacting residues (Figure 3E). The absence of Glu399 in the BD3 and BD4, Glu400 in the BD1, BD3, and BD4, Asp410 in the BD2, and Gln432 in the BD1, BD2, and BD4 is considered to be the reason why these BDs failed to bind the NBD, in spite of their high structural similarity to the BD5.

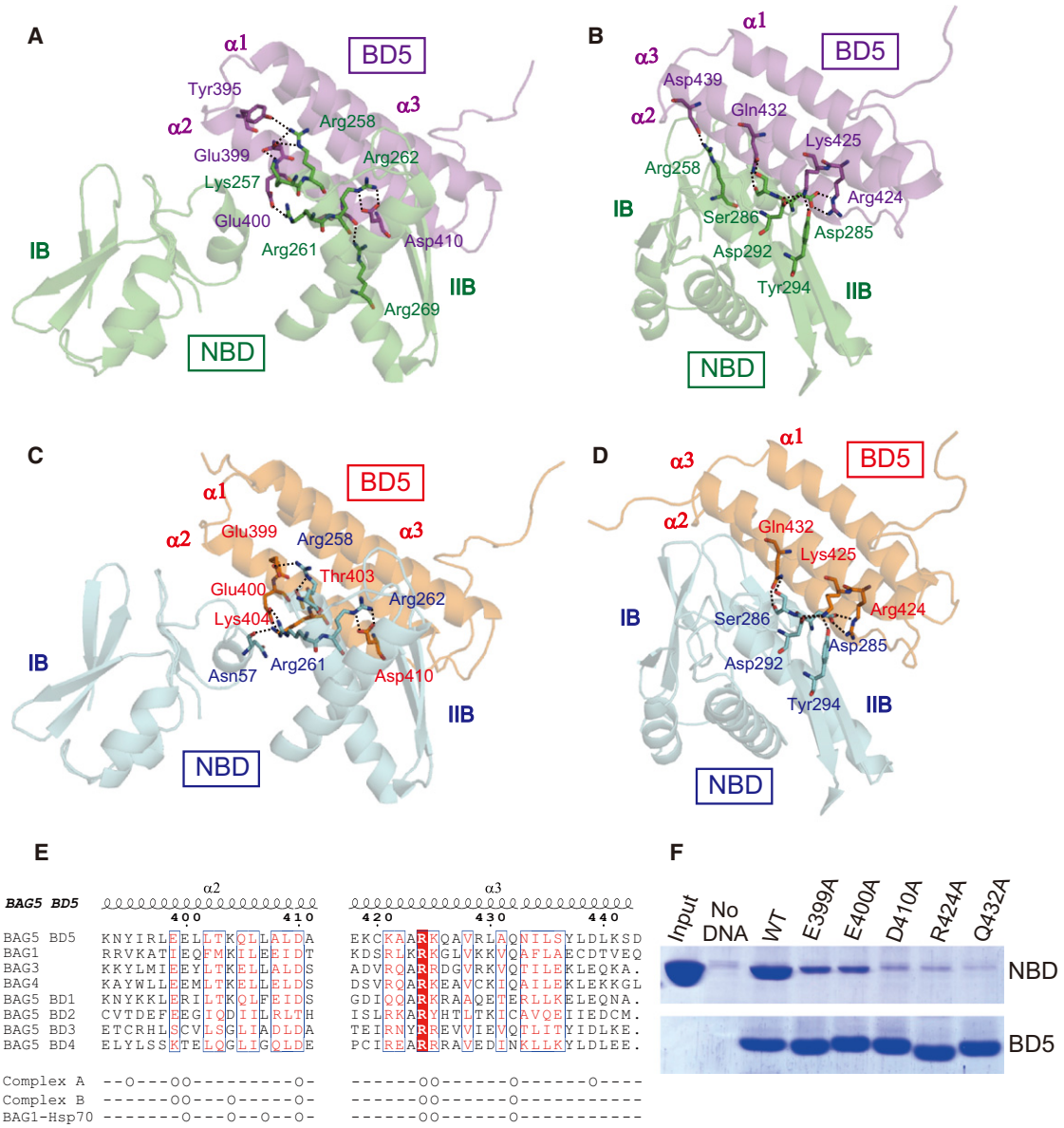

Figure 3. The Interacting Residues from the Hsp70 NBD and the BAG5 BD5

(A) Close-up view of the interaction between the NBD (green) and helix α2 of the BD5 (magenta) in complex A.

(B) Close-up view of the interaction between the NBD (green) and helix α3 of the BD5 (magenta) in complex A.

(C) Close-up view of the interaction between the NBD (cyan) and helix α2 of the BD5 (orange) in complex B.

(D) Close-up view of the interaction between the NBD (cyan) and helix α3 of the BD5 (orange) in complex B. All stick models indicate interacting residues.

(E) Sequence alignment of helices α2 and α3 in the BDs from human BAG1, BAG3, BAG4, and BAG5 and the positions of the interacting residues in the BDs from complexes A and B and the BAG1 BD•NBD complex (Sondermann et al., 2001).

(F) In vitro binding assay between the purified NBD and His-BD5 mutants. In the lane labeled "No DNA," the sample synthesized in the *Escherichia coli* cell-free protein expression system without DNA was used as a negative control.

Glu399 of the BAG5 BD5 is missing in the BAG1 BD, while it is conserved in BAG3 and BAG4. The corresponding residue of the BAG1 BD, Ile211, is not involved in the NBD binding (Sondermann et al., 2001). Therefore, it was suggested that the NBD-binding mechanism is not exactly the same between the BAG1 BD and the BAG4 BD (Brockmann et al., 2004), and this has now been unambiguously demonstrated by the present BD5•NBD complex structures. In the BAG1 BD, Glu219 interacts with Arg261 and Thr265 in the NBD. However, Glu219 of the BAG1 BD is not conserved in the BAG4 BD, BAG5 BD5, or BAG3 BD and corresponds to a conserved Leu residue (Leu407 in the BAG5 BD5) (Figure 3E). In fact, Leu407 of the BD5 is not involved in the NBD binding in the present structures. Therefore, it is likely that Glu399 (or its equivalent residue) in the short BDs functionally compensates for the lack of Glu residues in the other positions corresponding to Glu219 of the BAG1 BD.

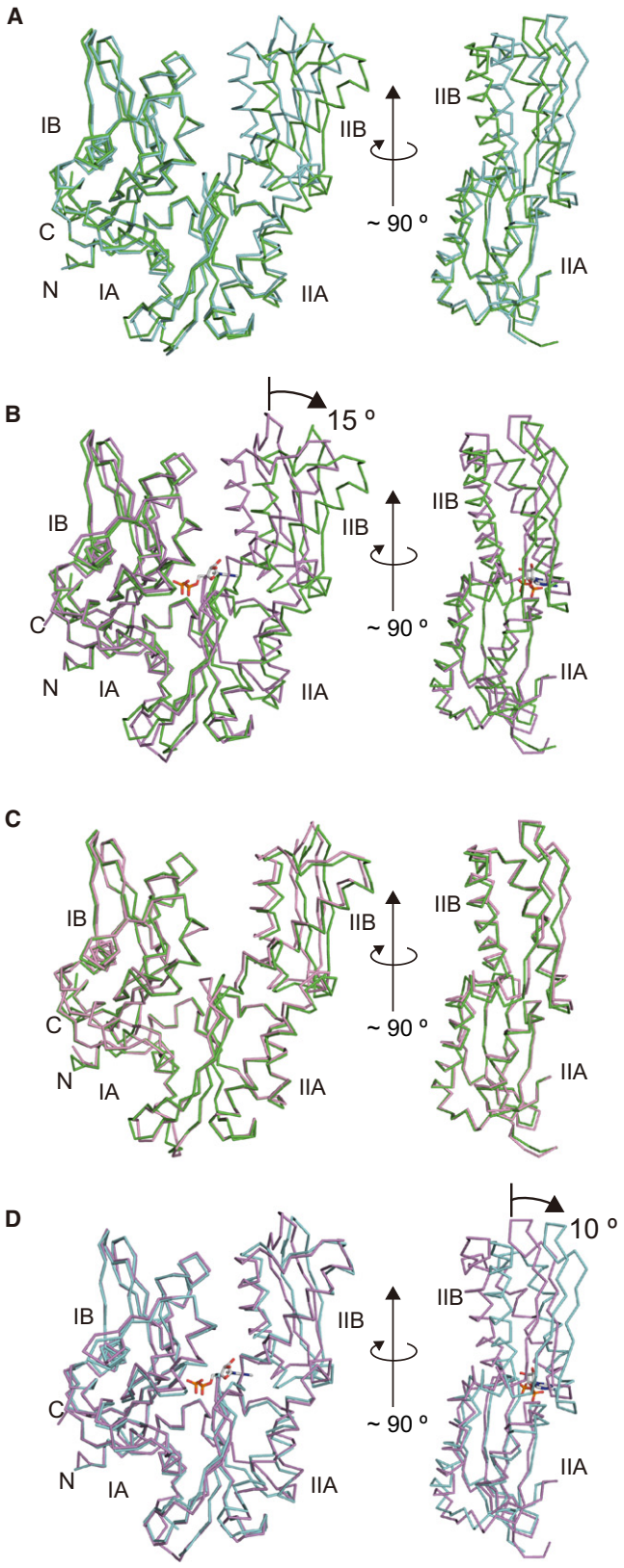

Figure 4. Comparison of Overall NBD Structures

(A) Comparison of the NBD structures in complexes A (green) and B (cyan).

(B) Comparison of the NBD structures in complex A and in the ADP-bound state (violet) (PDB ID: 1HJO) (Osipiuk et al., 1999).

(C) Comparison of the NBD structures in complex A and in the complex with the BAG1 BD (pink) (PDB ID: 1HX1) (Sondermann et al., 2001).

(D) Comparison of the NBD structures in complex B and in the ADP-bound state. White-based stick models represent ADP. All structural comparisons were performed by the superposition of subdomains IA, IB, and IIA, using the program LSQKAB (CCP4, 1994). As shown in Figures S2 and S3, we compared the NBD structures in complexes A and B with other reported NBD structures.

Comparison of the NBD Structures

The Hsp70 NBD is divided into four subdomains, IA (residues 1–39, 116–188, and 361–384), IB (residues 40–115), IIA (residues 189–228 and 307–360), and IIB (residues 229–306). The region between subdomains IIA and IIB is flexible, and subdomain IIB can rotate at this hinge region relative to the other subdomains (Bhattacharya et al., 2009; Xu et al., 2008). Therefore, to compare the NBD structures in complexes A and B, we superimposed their IA, IB, and IIA subdomains, using the program LSQKAB (CCP4, 1994). The position of subdomain IIB relative to the other three subdomains is apparently different between complexes A and B, in both the front and side views (Figure 4A).

In order to analyze these NBD structures, we compared each of them with previously reported NBD structures. First, we compared the structure of the NBD in complex A (NBD A) with that of the ADP-bound NBD (PDB ID: 1HJO) (Osipiuk et al., 1999). When an adenine nucleotide, such as ATP, ADP, and AMPPNP, binds to the NBD, the adenosine moiety interacts with subdomain IIB and the phosphate groups interact with subdomains IA, IB, and IIA. The nucleotide binding causes subdomains IB and IIB to approach each other, and the NBD structure adopts the closed state. In contrast, subdomain IIB is rotated by about 15° in the NBD A, as compared with that in the ADP-bound NBD (Figure 4B). Second, we compared the structure of the NBD A with that in the complex with the BAG1 BD (PDB ID: 1HX1) (Sondermann et al., 2001). As mentioned above, the structure of the NBD in the complex with the BAG1 BD is in the open state. The two NBD structures are very similar to each other, indicating that the structure of the NBD A is also in the open state (Figure 4C). In this context, an open-state structure of the NBD has also been reported for a longer fragment covering both the NBD and SBD of bovine Hsc70 (PDB ID: 1YUW) (Jiang et al., 2005), which is quite similar to the NBD structure in the BAG1 BD•NBD complex (Sondermann et al., 2001) (Figure S2A), as discussed in Shida et al. (2010). Actually, the present NBD A structure superimposed slightly better on the BAG1 BD•NBD structure than on the NBD-SBD structure (Figure S2B).

We next compared the structure of the NBD in complex B (NBD B) with that of the ADP-bound NBD. In the front view (Figure 4D, left), the NBD B appears to be similar to that of the ADP-bound NBD in the closed state. However, in the side view (Figure 4D, right), subdomain IIB is rotated by 10° in the NBD B, as compared with that in the ADP-bound NBD. Therefore, the NBD B structure is in a distorted state, rather than in the closed state (Figure 4D). Furthermore, the NBD B structure does not superpose well with those in the previously reported open-state structures: the Hsc70 NBD-SBD (PDB ID: 1YUW) (Jiang et al., 2005)

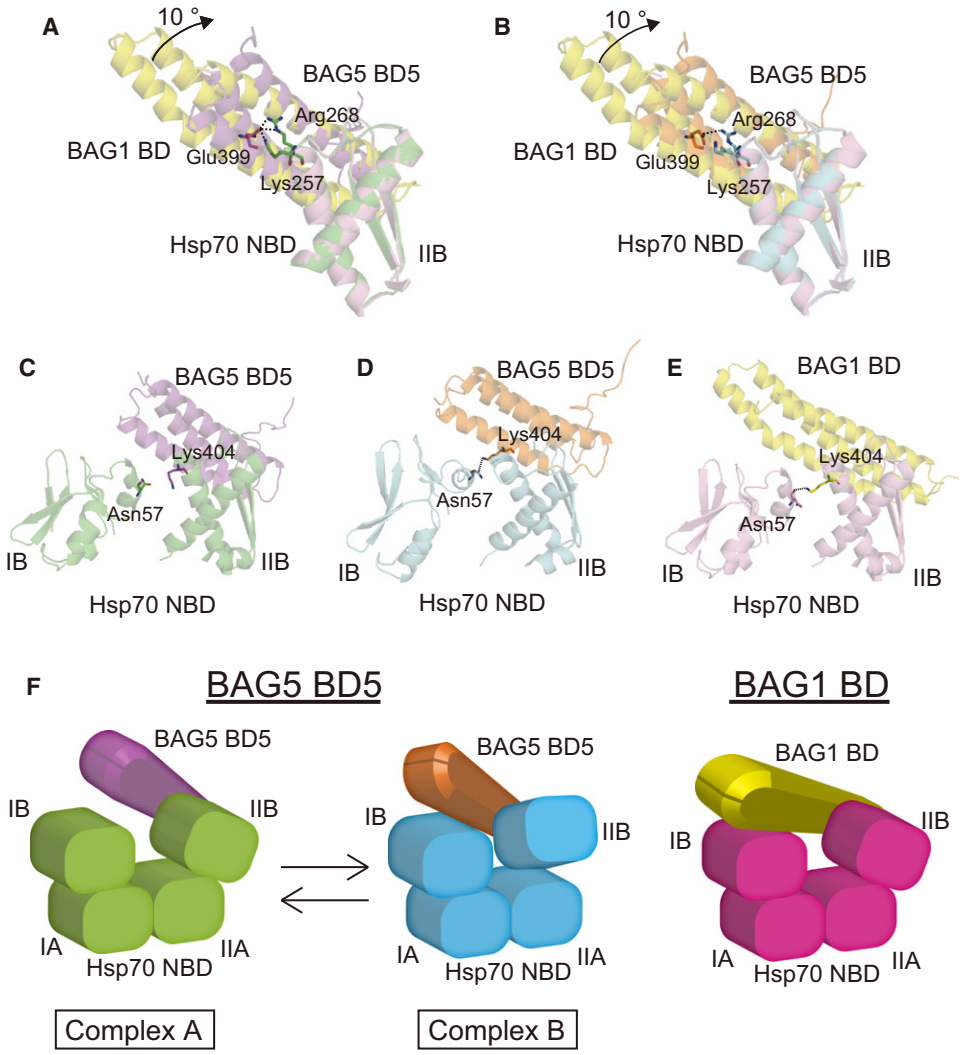

Figure 5. Structural Differences between the BD5•NBD and BAG1 BD•NBD Complexes

(A) Close-up view of Glu399 from the BD5 in complex A (NBD, green; BD5, magenta) and Ile211 from the BAG1 BD in the BAG1 BD•NBD complex (NBD, pink; BAG1 BD, yellow).

(B) Close-up view of Glu399 from the BD5 in complex A (NBD, cyan; BD5, orange) and Ile211 from the BAG1 BD in the BAG1 BD•NBD complex (NBD, pink; BAG1 BD, yellow). (A) and (B) were created by the superposition of subdomain IIB of the NBDs.

(C) Close-up view of Asn57 from the NBD and Lys404 from the BD5 in complex A.

(D) Close-up view of Asn57 from the NBD and Lys404 from the BD5 in complex B.

(E) Close-up view of Asn57 from the NBD and Lys404 from the BAG1 BD.

(F) Schematic models of the structures of the BD5•NBD and BAG1 BD•NBD complexes. As shown in Figure S4, the open state of the NBD A may be stabilized by a new hydrogen bond between Gly230 (subdomain IIB) and Ser340 (subdomain IIA).

(Figure S3A), the complex with the BAG2 BNB domain (PDB ID: 3CQX) (Xu et al., 2008) (Figure S3B), and the complex with Sse1 (PDB ID: 3D2F) (Polier et al., 2008) (Figure S3C). In summary, the NBD in the complex with the BD5 was observed in two states. In one state, the NBD structure assumes the open form similar to that in the complex with the BAG1 BD, and in the other state, the NBD structure assumes a novel, distorted form.

The Difference in the NBD-Binding Modes between BAG5 BD5 and BAG1 BD

We compared the NBD and BD residues involved in the interaction within the BAG1 BD•NBD complex, in which the NBD assumes the open form (Sondermann et al., 2001; Williamson et al., 2009), and in the BAG5 BD5•NBD complexes A and B in the open form and the distorted form, respectively. Glu399 in the BD5, which is conserved in the BAG3 and BAG4 BDs, but not in the BAG1 BD (Figure 3E), interacts with Lys257 and/or Arg258 in the NBD (Figures 3A and 3C). In contrast, the helix bundle of the BD5 is rotated by about 10° in complexes A and B, compared with its position in the BAG1 BD•NBD complex, as revealed by the superposition of these structures on subdomain IIB of the NBD (Figures 5A and 5B). The directional differences can be ascribed to the interaction through Glu399 in the BD5. In the BAG1 BD•NBD complex,

Lys216 (equivalent to Lys404 in BAG5 BD5) interacts with Asn57 in subdomain IB of the NBD in the open state (Figure 5C). However, because of the upper rotation of the helix bundle, Lys404 in the BD5 cannot reach Asn57 in subdomain IB in the NBD A, which assumes the typical open state (Figure 5D). Thus, the BD5 interacts only with subdomain IIB, but not at all with subdomain IB, in the NBD A. This open state may be stabilized by a new hydrogen bond between Gly230 (subdomain IIB) and Ser340 (subdomain IIA) within the NBD (Figure S4), as pointed out for the other open forms (Shida et al., 2010). In contrast, in the distorted state, Lys404 in the BD5 is still able to interact with Asn57 in subdomain IB in the NBD B (Figure 5E), while subdomains IIA and IIB do not acquire the hydrogen bond between Gly230 and Ser340. Therefore, the BD5 may stabilize the distorted state by interacting with both subdomains IB and IIB. In this context, the BAG1 BD can stabilize the open state of the NBD through interactions with both subdomains IB and IIB, as well as by the interaction between subdomains IIA and IIB (Shida et al., 2010). However, if the NBD in complex with the BD5 assumed the closed form, as in the ADP-bound NBD structure, then the BD5 would clash with subdomain IB. Consequently, the BAG5 BD5•NBD complex is likely to exist in an equilibrium between the open and distorted states, but not in the closed state (Figure 5F).

The Nucleotide-Binding Groove in the Open State (Complex A) and in the Distorted State (Complex B) of the BD5•NBD Complex

The NBD nucleotide-binding grooves in the open and distorted states of the BD5•NBD complex were examined in comparison with that in the closed state. In the ADP-bound NBD in the closed state, the adenosine moiety binds to Glu268, Lys271, and Ser275 in subdomain IIB, and the diphosphate moiety binds to Thr13, Thr14, and Tyr15 in subdomain IA and Gly339 in subdomain IIA. ADP brings subdomain IIB near subdomain IB and, simultaneously, the NBD retains the ADP by maintaining its closed state. In contrast, in complexes A and B, the adenosine-binding residues shift farther by 4 Å and 3 Å, respectively, from the diphosphate-binding residues, as compared with those in the ADP-bound NBD (Figure 6A). These results indicate that the NBD in the distorted state binds ADP only weakly, as in the case of that in the open state. Therefore, the BAG5 BD5 seems to accelerate the release of ADP from the NBD, either in the open state or in the distorted state. In other words, the BD5 and ADP compete with each other for binding to the NBD.

One of the possible scenarios of nucleotide exchange is as follows. First, the BD5 associates with the ADP-bound NBD and induces the distorted form through interactions with both subdomains IB and IIB. Then, after the ADP dissociation, the BD5 may disengage first from subdomain IB, as in the open form of the NBD A, which may be stabilized by the interaction between subdomains IIA and IIB. Finally, the BD5 dissociates from subdomain IIB, when ATP rebinds to the NBD and induces its closed form. In this scenario, the two states observed in complexes B and A would thus represent successive states in the conformational trajectory of the NBD upon interaction with the BD5.

BD5 Functions as the Nucleotide Exchange Factor of Hsp70

We demonstrated the effect of the BD5 on the affinity of the NBD for ADP by an isothermal titration calorimetry (ITC) assay. We titrated the NBD fragment solution (10 μM) with the ADP solution (400 μM) and obtained an affinity of 42.7 nM and a stoichiometry factor of approximately 1 (Figure 6B). Next, we titrated the BD5•NBD complex solution (10 μM) with the ADP solution (400 μM). The curve of heat changes was fitted using a one-site binding model and demonstrated an affinity of 508 nM and a stoichiometry factor of approximately 1 (Figure 6C). This indicated that the presence of the BD5 reduced the affinity of the NBD for ADP. The BD5 also reduced the affinity of the NBD for ATP. Nevertheless, ATP is present in an excess amount in the cytosol and may still bind to the BD5•NBD complex. Actually, an in vitro pull-down assay revealed that an excess amount of ATP dissociated the BD5 from the NBD (Figure 6D). Therefore, the BD5 promotes the release of ADP and the entry of ATP, by disrupting the nucleotide-binding groove in the NBD.

In order to examine the effect of the BD5 on the chaperone activity of Hsp70, we refolded heat-denatured luciferase with Hsp70 in vitro and added the BD5 to the refolding reaction. The addition of the BD5 noticeably increased the luciferase activity (Figure 6E). Next, we added the D410A mutant of the BD5, which was defective in binding to the NBD in our pull-down assay, to the refolding reaction. As a result, the addition of the BD5 mutant did not increase the luciferase activity (Figure 6E). Therefore, the BD5 activates the Hsp70-mediated refolding by enhancing the exchange of ADP to ATP. That is, the BD5 functions as the NEF of Hsp70.

BD5 Is Responsible for the Function of BAG5 with Hsp70

Finally, we examined the effect of the full-length BAG5, with the BD1–BD5, on the Hsp70 chaperone activity. As in the case of the BD5, the full-length BAG5 with the D410A mutation was unable to associate with the NBD (Figure 7A). Consequently, the BD5, but not the other BDs, is responsible for the binding of BAG5 with the NBD. Furthermore, the refolding of heat-denatured luciferase by Hsp70 in vitro was enhanced by BAG5, but not by its D410A mutant (Figure 7B). Therefore, BAG5 enhances the Hsp70 chaperone activity through the interaction of its BD5 with the NBD.

In summary, our biochemical assays and the crystal structure of the BD5•NBD complex revealed that BAG5 interacts with the Hsp70 NBD through the BD5, facilitates the unique conformational change in the NBD, promotes the ADP release and the ATP entry, and activates the Hsp70-mediated refolding in vitro. Thus, we concluded that BAG5 activates Hsp70-mediated refolding, as the NEF (Figure 7C). BAG5 is usually expressed in various tissues, and cellular injury induces BAG5 expression (Kalia et al., 2004), which suggests that the role of BAG5 in the normal cells is to assist the cellular Hsp70 chaperone system. This molecular function of BAG5 should be taken into account to understand how overexpression of BAG5 causes protein aggregation in dopaminergic neurons and the neurodegeneration associated with endoplasmic reticulum stress (Chung and Dawson, 2004; Kalia et al., 2004).

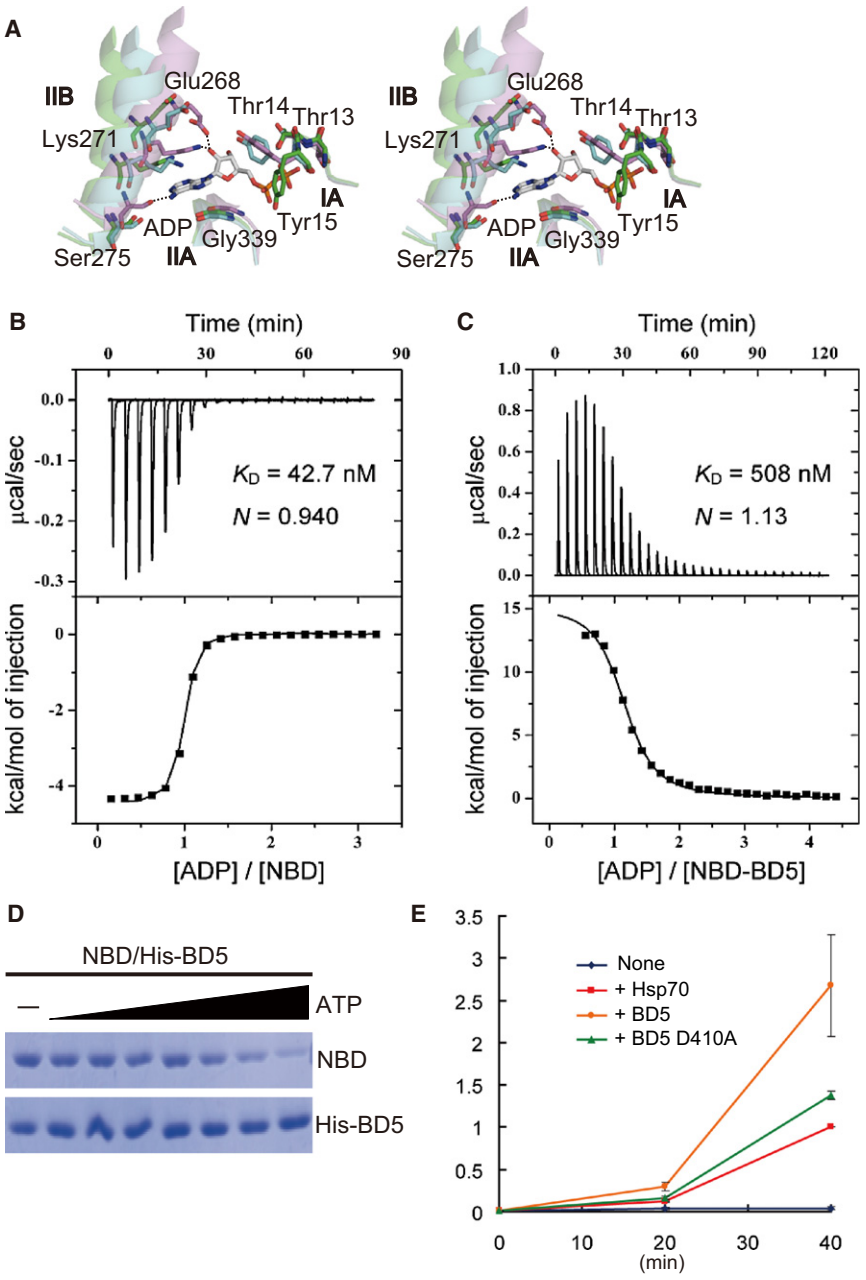

Figure 6. Mechanism of the BD5-Mediated Nucleotide Exchange

(A) Stereo view of the nucleotide-binding grooves of the NBD A (green), the NBD B (cyan), and the ADP-bound state (violet). The white-based stick model represents ADP, and the other stick models indicate ADP-interacting residues.

(B) ITC analysis of the interaction of the Hsp70 NBD with ADP.

(C) ITC analysis of the interaction of the NBD with ADP in the presence of the BAG5 BD5.

(D) In vitro pull-down assay between the NBD and His-BD5 in the presence of ATP. The concentrations of ATP in lanes 1–8 are 0 M, 5 μM, 10 μM, 20 μM, 40 μM, 80 μM, 160 μM, and 1 mM, respectively.

(E) Effect of the BAG5 BD5 on Hsp70-mediated refolding activity, measured by denatured luciferase. "None" indicates the activity of denatured luciferase incubated with no chaperone. "Hsp70" indicates the activity of denatured luciferase incubated with Hsp70 and Hsp40. "+ BD5 WT" indicates the activity of denatured luciferase incubated with Hsp70, Hsp40, and the BAG5 BD5. "+ BD5 D410A" indicates the activity of denatured luciferase incubated with Hsp70, Hsp40, and the D410A mutant of the BAG5 BD5. The activity of luciferase incubated with Hsp70 and Hsp40 for 40 min was set to 1 and n = 5. The error bars represent the standard errors.

EXPERIMENTAL PROCEDURES

Expression Vectors

The DNA regions encoding human Hsp70, the NBD (residues 1–388), and Hsp40 were cloned into pENTR/TEV/D-TOPO (Invitrogen). Their expression vectors were constructed using GATEWAY technology (Invitrogen) with the pET-32/GATEWAY vector, which was inserted into the GATEWAY reading frame cassette A (Invitrogen) in pET-32a (+) (Novagen) (Shida et al., 2010).

The DNA regions encoding human BAG5 FL, BD1 (residues 1–86), BD2–3 (residues 86–260), BD4 (residues 275–350), and BD5 (residues 341–447 and residues 361–447) and murine BAG5 BD1 (residues 1–86) and BAG3 BD (residues 406–503), as the N-terminal fusion with a histidine affinity tag, a tobacco etch virus (TEV) protease cleavage site, and seven extra residues (GSSGSSG), were cloned into the pCR2.1-TOPO vector using a TOPO TA cloning kit (Invitrogen). The point mutations of the BAG5 FL and BD5 were introduced using QuickChange (Stratagene) mutagenesis and were verified by DNA sequencing.

In Vitro Pull-down Assay

The expression of human BAG5 FL, BD1 (residues 1–89), BD2–3 (residues 86–260), BD4 (residues 275–350), and BD5 (residues 341–447) and the D410A mutants of the BAG5 FL and BD5 was accomplished with the *Escherichia coli* cell-free protein expression system (Kigawa et al., 2004, 2007) at 30°C for 4 hr. After cell-free synthesis, the reaction solutions were clarified by centrifugation. ProBond Nickel-Chelating Resin (Invitrogen), equilibrated with wash buffer [25 mM sodium phosphate buffer (pH 8.0) containing 150 mM NaCl and 10 mM imidazole], was mixed with the supernatants, washed with the wash buffer, and then mixed with the NBD and purified as described below. After incubating the mixture at 4°C for 2 hr and washing with the wash buffer, the proteins bound to the resins were eluted with elution buffer [25 mM sodium phosphate buffer (pH 8.0) containing 150 mM NaCl and 200 mM imidazole]. Finally, we performed SDS-PAGE and CBB staining to detect the NBD.

Purification of the BD5•NBD Complex

The expression of the Hsp70 NBD was performed in *Escherichia coli* Rosetta2 (DE3) cells by induction with 0.5 mM IPTG overnight at 18°C, and the expression of the BAG5 BD5 was performed in *Escherichia coli* KRX cells by induction with 0.1% rhamnose overnight at 18°C.

Next, we purified the BAG5 BD5 (residues 341–447) and Hsp70 NBD separately. The cells were harvested by centrifugation and suspended in 20 mM Tris-HCl buffer (pH 8.0), containing 500 mM NaCl, 5 mM imidazole, and 5 mM β-mercaptoethanol. The cells were lysed by sonication and cleared by centrifugation and filtration. The clarified lysates were loaded on a HisTrap

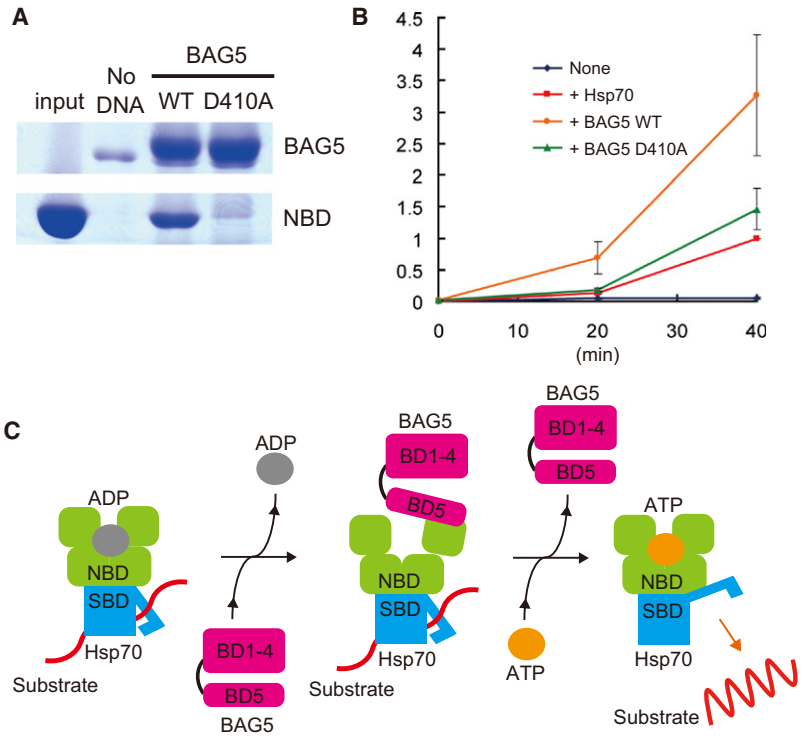

Figure 7. The Effect of BAG5 on Hsp70 Chaperone Activity

(A) In vitro pull-down assay, using the His-tagged BAG5 FL and the D410A mutant and the purified Hsp70 NBD. In the lane labeled "No DNA," the sample synthesized in the *Escherichia coli* cell-free protein expression system without DNA was used as a negative control.

(B) Effect of BAG5 on Hsp70-mediated refolding activity, measured by denatured luciferase. "None" indicates the activity of denatured luciferase incubated with no chaperone. "Hsp70" indicates the activity of denatured luciferase incubated with Hsp70 and Hsp40. "+ BAG5 WT" indicates the activity of denatured luciferase incubated with Hsp70, Hsp40, and the BAG5 FL. "+ BAG5 D410A" indicates the activity of denatured luciferase incubated with Hsp70, Hsp40, and the D410A mutant of the BAG5 FL. The activity of luciferase incubated with Hsp70 and Hsp40 for 40 min was set to 1 and n = 5. The error bars represent the standard errors.

(C) Schematic models of the nucleotide exchange mechanism of BAG5.

column (GE Healthcare) and were eluted with an imidazole gradient from 5 mM to 500 mM. Fractions containing the BD5 or NBD protein were pooled separately, and TEV protease was added to the protein solutions. The samples were dialyzed against 20 mM Tris-HCl buffer (pH 8.0), containing 25 mM NaCl and 5 mM β-mercaptoethanol, overnight at 4°C. After centrifugation and filtration, the clarified samples were loaded on the HisTrap column again to remove the TEV protease and the cleaved His tag. The samples were then loaded on a Resource Q column (GE Healthcare) and eluted with an NaCl gradient from 25 mM to 1 M. The fractions containing the BD5 or NBD protein were pooled, concentrated to less than 5 ml by centrifugation in an Amicon ultra filter (Millipore), filtered, loaded on a HiLoad 16/60 Superdex 200 column (GE Healthcare), and eluted with 20 mM Tris-HCl buffer (pH 8.0), containing 150 mM NaCl and 5 mM β-mercaptoethanol.

After purifying the NBD and BD5 proteins separately, we mixed them in a one to one ratio and incubated the solution at 4°C for 2 hr. This sample was loaded on a HiLoad 16/60 Superdex 200 column and eluted with 20 mM Tris-HCl buffer (pH 8.0), containing 150 mM NaCl and 5 mM β-mercaptoethanol, and the fractions containing the BD5•NBD complex were pooled.

Crystallization, Data Collection, Model Building, and Refinement

The protein sample was concentrated to 5.5 mg/ml and was crystallized by the hanging drop vapor diffusion method at 293 K against a reservoir solution [0.1 M Tris-HCl buffer (pH 8.0) containing 20% PEG MME 2000, 0.25 M trimethylamine N-oxide, and 3% hexanediol]. The crystal belongs to the space group $P2_1$, with unit-cell parameters a = 64.11 Å, b = 84.27 Å, c = 96.63 Å, $\alpha = \gamma = 90.0°$, and $\beta = 100.7°$, and there are two BD5•NBD complexes in the asymmetric unit.

All diffraction data were recorded at 100 K, with the reservoir solution containing 15% glycerol as a cryoprotectant. X-ray diffraction data were collected at a 1.0 Å wavelength at BL26B2 of SPring-8 and were processed with the HKL2000 and SCALEPACK programs (Otwinowski and Minor, 1997).

The crystal structure of the BD5•NBD complex was determined by the molecular replacement method, using the MOLREP program (Vagin and Teplyakov, 1997). The NBD structure in the complex with the BAG1 BD (PDB ID: 1HX1) (Sondermann et al., 2001) and the BD5 structure created by SWISS-MODEL were used as the search models. After several rounds of manual revisions of the model using the TURBO-FRODO program and refinements using the CNS programs (BrÜnger et al., 1998), the R_{work} and R_{free} were 21.8% and 28.1%, respectively, and the refined structure had no Ramachandran violations, as examined by the PROCHECK program (Laskowski et al., 1996). Crystallographic data collection and refinement statistics are summarized in Table 1. The crystal structure of the BD5•NBD complex has been deposited in the Protein Data Bank (PDB code: 3A8Y).

NMR Spectroscopy, Structure Determination, and Analysis

All of the NMR spectra were recorded at 25°C on Varian INOVA 600, 800, and 900 spectrometers equipped with pulse-field gradient triple-resonance probes. Sequence-specific resonance assignments were made using the standard triple-resonance techniques. The backbone assignment was achieved by the combined analysis of HNCO, (HCA)CO(CA)NH, HN(CO)CA, HNCACB, and CBCA(CO)NH spectra. The side-chain resonances were identified by the combined use of HBHANH, HBHA(CO)NH, (H)CC(CO)NH, (H)CCH-TOCSY, HCCH-TOCSY, and two-dimensional ^{1}H-^{15}N HSQC and ^{1}H-^{13}C HSQC spectra. NOE data for structure determination were extracted from three-dimensional ^{15}N- and ^{13}C-edited NOESY spectra, recorded with mixing times of 75 and 65 ms, respectively, for BAG5 BD4, and 75ms for both BAG3 BD and BAG5 BD1. The NMRPipe software package (Delaglio et al., 1995) and the program KUJIRA (Kobayashi et al., 2007), created on the basis of NMRView (Johnson and Blevins, 1994), were used for optimal visualization and spectral analysis. Automated NOE cross-peak assignments (Herrmann et al., 2002) and structure calculations with torsion angle dynamics were performed using the software package CYANA1.0.7 for BAG3 BD and BAG5 BD1 and CYANA2.0.17 for BAG5 BD4 (GÜntert, 2003).

Dihedral angle restraints were derived using the program TALOS (Cornilescu et al., 1999). A total of 100 conformers were calculated independently. The 20 conformers with the lowest final CYANA target function values were finally selected. The structures were validated using PROCHECK-NMR (Laskowski et al., 1996). The program MOLMOL (Koradi et al., 1996) was used to analyze the resulting 20 conformers. The selected 20 conformers have been deposited in the Protein Data Bank (PDB codes: 1UK5 for BAG3 BD, 1UGO for BAG5 BD1, and 2D9D for BAG5 BD4).

ITC Measurements

The interaction between the NBD and ADP was monitored by ITC measurements (Wiseman et al., 1989), performed at 25°C with a Microcal VP-ITC calorimeter. Samples were buffered with 20 mM Tris-HCl buffer (pH 8.0), containing 150 mM NaCl, 5 mM $MgCl_2$, and 1 mM DTT. Aliquots of a 400 μM ADP solution (syringe) were stepwise injected into a 10 μM NBD solution with or

Table 1. Crystallographic Data and Refinement Statistics

	The BD5•NBD Complex
Data collection	
Beamline	SPring-8 BL26B2
Space group	$P2_1$
Unit cell	
a, *b*, *c* (Å)	64.11, 84.27, 96.63
α, β, γ (°)	90.0, 100.7, 90.0
Resolution (Å)	50–2.30 (2.38–2.30)[a]
No. of measured reflections	118,991
No. of unique reflections	42,589
Redundancy	2.79
Completeness (%)	94.5 (85.2)[a]
I/σ (I)	21.2 (4.1)[a]
R_{sym}[b] (%)	4.7 (18.1)[a]
Refinement statistics	
Resolution (Å)	19.98–2.30
No. of reflections	42,522
No. of protein atoms	2,134
No. of Tris molecules	2
No. of water molecules	522
R_{work}/R_{free}[c] (%)	21.8/28.1
Rmsd bond length (Å)	0.006
Rmsd bond angles (°)	1.2
Average isotropic B value (Å^2)	40.2
Ramachandran plot	
Most favored regions (%)	86.3
Additional allowed regions (%)	13.4
Generously allowed regions (%)	0.3
Disallowed regions (%)	0
PDB code	3A8Y

[a] Statistics for the highest resolution shell are given in parentheses.
[b] $R_{sym} = \Sigma|I - < I >|/\Sigma I$, where I is the observed intensity of reflections.
[c] R_{work}, $R_{free} = \Sigma|F_{obs} - F_{calc}|/\Sigma F_{obs}$, where the crystallographic R factor is calculated including and excluding refinement reflections. In each refinement, free reflections consist of 5% of the total number of reflections.

without 10 μM BD5 protein (cell). The heat generated due to the dilution of the ADP solution was quite small and was ignored for the analysis. The data were analyzed with the Microcal ORIGIN software, using a binding model that assumes a single site of interaction.

Refolding Assay

Luciferase (13 mg/ml) (Promega) was diluted 42-fold with 30 mM HEPES-NaOH buffer (pH 7.5), containing 50 mM KCl, 6 M Urea, and 10 mM $MgCl_2$, and was denatured at 42°C for 30 min. The denatured luciferase was diluted 250-fold with 30 mM HEPES-NaOH and 1 mM Tris-HCl buffer (pH 7.5), containing 50 mM KCl, 10 mM $MgCl_2$, 2 mM DTT, 1 μM Hsp70, 2 μM Hsp40, and 0.2 μM of the BAG5 FL, BD5, and their mutants, and was refolded at 30°C. The luciferase activity was determined with a Luciferase assay kit (Promega).

ACCESSION NUMBERS

Coordinates have been deposited in the Protein Data Bank, under the accession numbers 1UGO (BAG5 BD1), 1UK5 (BAG3 BD), 2D9D (BAG5 BD4), and 3A8Y (BD5•NBD complex).

SUPPLEMENTAL INFORMATION

Supplemental Information includes four figures and Supplemental Experimental Procedures and can be found with this article online at doi:10.1016/j.str.2010.01.004.

ACKNOWLEDGMENTS

We thank Tetsuo Takagi, Atsushi Shimada, Seisuke Yamashita, Kazushige Katsura, and Takuma Kasai for helpful advice. We thank Mitsutoshi Toyama for the preparation of some expression vectors. We thank Takashi Umehara, Hideaki Niwa, and Ryogo Akasaka for X-ray diffraction data collection. We thank Takaho Terada and Makoto Inoue for sample preparation for NMR analysis. We are grateful to the beamline staff at BL26B2 at SPring-8 (Hyogo, Japan) for assistance with our X-ray data collection. This work was supported by the Targeted Proteins Research Program from the Ministry of Education, Culture, Sports, Science and Technology of Japan.

Received: October 20, 2009
Revised: January 7, 2010
Accepted: January 11, 2010
Published: March 9, 2010

REFERENCES

Andreasson, C., Fiaux, J., Rampelt, H., Mayer, M.P., and Bukau, B. (2008). Hsp110 is a nucleotide-activated exchange factor for Hsp70. J. Biol. Chem. *283*, 8877–8884.

Bhattacharya, A., Kurochkin, A.V., Yip, G.N., Zhang, Y., Bertelsen, E.B., and Zuiderweg, E.R. (2009). Allostery in Hsp70 chaperones is transduced by subdomain rotations. J. Mol. Biol. *388*, 475–490.

Bimston, D., Song, J., Winchester, D., Takayama, S., Reed, J.C., and Morimoto, R.I. (1998). BAG-1, a negative regulator of Hsp70 chaperone activity, uncouples nucleotide hydrolysis from substrate release. EMBO J. *17*, 6871–6878.

Briknarová, K., Takayama, S., Brive, L., Havert, M.L., Knee, D.A., Velasco, J., Homma, S., Cabezas, E., Stuart, J., Hoyt, D.W., et al. (2001). Structural analysis of BAG1 cochaperone and its interactions with Hsc70 heat shock protein. Nat. Struct. Biol. *8*, 349–352.

Briknarová, K., Takayama, S., Homma, S., Baker, K., Cabezas, E., Hoyt, D.W., Li, Z., Satterthwait, A.C., and Ely, K.R. (2002). BAG4/SODD protein contains a short BAG domain. J. Biol. Chem. *277*, 31172–31178.

Brockmann, C., Leitner, D., Labudde, D., Diehl, A., Sievert, V., Buessow, K., Kuhne, R., and Oschkinat, H. (2004). The solution structure of the SODD BAG domain reveals additional electrostatic interactions in the HSP70 complexes of SODD subfamily BAG domains. FEBS Lett. *558*, 101–106.

BrÜnger, A.T., Adams, P.D., Clore, G.M., DeLano, W.L., Gros, P., Grosse-Kunstleve, R.W., Jiang, J.S., Kuszewski, J., Nilges, M., Pannu, N.S., et al. (1998). Crystallography & NMR system: a new software suite for macromolecular structure determination. Acta Crystallogr. D Biol. Crystallogr. *54*, 905–921.

Bukau, B., and Horwich, A.L. (1998). The Hsp70 and Hsp60 chaperone machines. Cell *92*, 351–366.

Bukau, B., Weissman, J., and Horwich, A. (2006). Molecular chaperones and protein quality control. Cell *125*, 443–451.

Collaborative Computational Project, Number 4. (1994). The CCP4 suite: programs for protein crystallography. Acta Crystallogr. D Biol. Crystallogr. *50*, 760–763.

Chung, K.K., and Dawson, T.M. (2004). Parkin and Hsp70 sacked by BAG5. Neuron *44*, 899–901.

Cornilescu, G., Delaglio, F., and Bax, A. (1999). Protein backbone angle restraints from searching a database for chemical shift and sequence homology. J. Biomol. NMR *13*, 289–302.

Delaglio, F., Grzesiek, S., Vuister, G., Zhu, G., Pfeifer, J., and Bax, A. (1995). NMRPipe: a multidimensional spectral processing system based on UNIX pipes. J. Biomol. NMR *6*, 277–293.

Dragovic, Z., Broadley, S.A., Shomura, Y., Bracher, A., and Hartl, F.U. (2006). Molecular chaperones of the Hsp110 family act as nucleotide exchange factors of Hsp70s. EMBO J. *25*, 2519–2528.

Gassler, C.S., Wiederkehr, T., Brehmer, D., Bukau, B., and Mayer, M.P. (2001). Bag-1M accelerates nucleotide release for human Hsc70 and Hsp70 and can act concentration-dependent as positive and negative cofactor. J. Biol. Chem. *276*, 32538–32544.

GÜntert, P. (2003). Automated NMR protein structure calculation. Prog. Nucleic Magn. Reson. Spectrosc. *43*, 105–125.

Hartl, F.U., and Hayer-Hartl, M. (2002). Molecular chaperones in the cytosol: from nascent chain to folded protein. Science *295*, 1852–1858.

Harrison, C.J., Hayer-Hartl, M., Di Liberto, M., Hartl, F.U., and Kuriyan, J. (1997). Crystal structure of the nucleotide exchange factor GrpE bound to the ATPase domain of the molecular chaperone DnaK. Science *276*, 431–435.

Herrmann, T., GÜntert, P., and Wuthrich, K. (2002). Protein NMR structure determination with automated NOE assignment using the new software CANDID and the torsion angle dynamics algorithm DYANA. J. Mol. Biol. *319*, 209–227.

Höhfeld, J., and Jentsch, S. (1997). GrpE-like regulation of the hsc70 chaperone by the anti-apoptotic protein BAG-1. EMBO J. *16*, 6209–6216.

Jiang, J., Prasad, K., Lafer, E.M., and Sousa, R. (2005). Structural basis of interdomain communication in the Hsc70 chaperone. Mol. Cell *20*, 513–524.

Johnson, B., and Blevins, R. (1994). NMRView: a computer program for the visualization and analysis of NMR data. J. Biomol. NMR *4*, 603–614.

Kabani, M., McLellan, C., Raynes, D.A., Guerriero, V., and Brodsky, J.L. (2002). HspBP1, a homologue of the yeast Fes1 and Sls1 proteins, is an Hsc70 nucleotide exchange factor. FEBS Lett. *531*, 339–342.

Kabbage, M., and Dickman, M.B. (2008). The BAG proteins: a ubiquitous family of chaperone regulators. Cell. Mol. Life Sci. *65*, 1390–1402.

Kalia, S.K., Lee, S., Smith, P.D., Liu, L., Crocker, S.J., Thorarinsdottir, T.E., Glover, J.R., Fon, E.A., Park, D.S., and Lozano, A.M. (2004). BAG5 inhibits parkin and enhances dopaminergic neuron degeneration. Neuron *44*, 931–945.

Kigawa, T., Yabuki, T., Matsuda, N., Matsuda, T., Nakajima, R., Tanaka, A., and Yokoyama, S. (2004). Preparation of Escherichia coli cell extract for highly productive cell-free protein expression. J. Struct. Funct. Genomics *5*, 63–68.

Kigawa, T., Matsuda, T., Yabuki, T., and Yokoyama, S. (2007). Bacterial cell-free system for highly efficient protein synthesis. In Cell-free Protein Synthesis, A.S. Spirin and J.R. Swartz, eds. (Weinheim, Germany: WILEY-VCH), pp. 83–97.

Kobayashi, N., Iwahara, J., Koshiba, S., Tomizawa, T., Tochio, N., GÜntert, P., Kigawa, T., and Yokoyama, S. (2007). KUJIRA, a package of integrated modules for systematic and interactive analysis of NMR data directed to high-throughput NMR structure studies. J. Biomol. NMR *39*, 31–52.

Koradi, R., Billeter, M., and Wuthrich, K. (1996). MOLMOL: a program for display and analysis of macromolecular structures. J. Mol. Graph. *14*, 51–55.

Laskowski, R.A., Rullmann, J.A., MacArthur, M.W., Kaptein, R., and Thornton, J.M. (1996). AQUA and PROCHECK-NMR: programs for checking the quality of protein structures solved by NMR. J. Biomol. NMR *8*, 477–486.

Liberek, K., Marszalek, J., Ang, D., Georgopoulos, C., and Zylicz, M. (1991). Escherichia coli DnaJ and GrpE heat shock proteins jointly stimulate ATPase activity of DnaK. Proc. Natl. Acad. Sci. USA *88*, 2874–2878.

Mayer, M.P., and Bukau, B. (2005). Hsp70 chaperones: cellular functions and molecular mechanism. Cell. Mol. Life Sci. *62*, 670–684.

Misselwitz, B., Staeck, O., and Rapoport, T.A. (1998). J proteins catalytically activate Hsp70 molecules to trap a wide range of peptide sequences. Mol. Cell *2*, 593–603.

Nollen, E.A., Kabakov, A.E., Brunsting, J.F., Kanon, B., Höhfeld, J., and Kampinga, H.H. (2001). Modulation of in vivo HSP70 chaperone activity by Hip and Bag-1. J. Biol. Chem. *276*, 4677–4682.

Osipiuk, J., Walsh, M.A., Freeman, B.C., Morimoto, R.I., and Joachimiak, A. (1999). Structure of a new crystal form of human Hsp70 ATPase domain. Acta Crystallogr. D Biol. Crystallogr. *55*, 1105–1107.

Otwinowski, Z., and Minor, W. (1997). Processing of X-ray diffraction data collected in oscillation mode. Methods Enzymol. *276*, 307–326.

Polier, S., Dragovic, Z., Hartl, F.U., and Bracher, A. (2008). Structural basis for the cooperation of Hsp70 and Hsp110 chaperones in protein folding. Cell *133*, 1068–1079.

Raviol, H., Sadlish, H., Rodriguez, F., Mayer, M.P., and Bukau, B. (2006). Chaperone network in the yeast cytosol: Hsp110 is revealed as an Hsp70 nucleotide exchange factor. EMBO J. *25*, 2510–2518.

Schuermann, J.P., Jiang, J., Cuellar, J., Llorca, O., Wang, L., Gimenez, L.E., Jin, S., Taylor, A.B., Demeler, B., Morano, K.A., et al. (2008). Structure of the Hsp110:Hsc70 nucleotide exchange machine. Mol. Cell *31*, 232–243.

Shaner, L., Sousa, R., and Morano, K.A. (2006). Characterization of Hsp70 binding and nucleotide exchange by the yeast Hsp110 chaperone Sse1. Biochemistry *45*, 15075–15084.

Shida, M., Arakawa, A., Ishii, R., Kishishita, S., Takagi, T., Kukimoto-Niino, M., Sugano, S., Tanaka, A., Shirouzu, M., and Yokoyama, S. (2010). Direct inter-subdomain interactions switch between the closed and open forms of the Hsp70 nucleotide-binding domain in the nucleotide-free state. Acta Crystallogr. D Biol. Crystallogr., in press.

Shomura, Y., Dragovic, Z., Chang, H.C., Tzvetkov, N., Young, J.C., Brodsky, J.L., Guerriero, V., Hartl, F.U., and Bracher, A. (2005). Regulation of Hsp70 function by HspBP1: structural analysis reveals an alternate mechanism for Hsp70 nucleotide exchange. Mol. Cell *17*, 367–379.

Sondermann, H., Scheufler, C., Schneider, C., Höhfeld, J., Hartl, F.U., and Moarefi, I. (2001). Structure of a Bag/Hsc70 complex: convergent functional evolution of Hsp70 nucleotide exchange factors. Science *291*, 1553–1557.

Takayama, S., and Reed, J.C. (2001). Molecular chaperone targeting and regulation by BAG family proteins. Nat. Cell Biol. *3*, E237–E241.

Takayama, S., Sato, T., Krajewski, S., Kochel, K., Irie, S., Millan, J.A., and Reed, J.C. (1995). Cloning and functional analysis of BAG-1: a novel Bcl-2-binding protein with anti-cell death activity. Cell *80*, 279–284.

Takayama, S., Bimston, D.N., Matsuzawa, S., Freeman, B.C., Aime-Sempe, C., Xie, Z., Morimoto, R.I., and Reed, J.C. (1997). BAG-1 modulates the chaperone activity of Hsp70/Hsc70. EMBO J. *16*, 4887–4896.

Takayama, S., Xie, Z., and Reed, J.C. (1999). An evolutionarily conserved family of Hsp70/Hsc70 molecular chaperone regulators. J. Biol. Chem. *274*, 781–786.

Thress, K., Henzel, W., Shillinglaw, W., and Kornbluth, S. (1998). Scythe: a novel reaper-binding apoptotic regulator. EMBO J. *17*, 6135–6143.

Vagin, A., and Teplyakov, A. (1997). MOLREP: an automated program for molecular replacement. J. Appl. Crystallogr. *30*, 1022–1025.

Walsh, P., Bursac, D., Law, Y.C., Cyr, D., and Lithgow, T. (2004). The J-protein family: modulating protein assembly, disassembly and translocation. EMBO Rep. *5*, 567–571.

Williamson, D.S., Borgognoni, J., Clay, A., Daniels, Z., Dokurno, P., Drysdale, M.J., Foloppe, N., Francis, G.L., Graham, C.J., Howes, R., et al. (2009). Novel adenosine-derived inhibitors of 70 kDa heat shock protein, discovered through structure-based design. J. Med. Chem. *52*, 1510–1513.

Wiseman, T., Williston, S., Brandts, J.F., and Lin, L.N. (1989). Rapid measurement of binding constants and heats of binding using a new titration calorimeter. Anal. Biochem. *179*, 131–137.

Xu, Z., Page, R.C., Gomes, M.M., Kohli, E., Nix, J.C., Herr, A.B., Patterson, C., and Misra, S. (2008). Structural basis of nucleotide exchange and client binding by the Hsp70 cochaperone Bag2. Nat. Struct. Mol. Biol. *15*, 1309–1317.